ARTICLE

Transfer-Free Batch Fabrication of Large-Area Suspended Graphene Membranes

Benjamín Alemán,[†,‡,§,#] William Regan,[†,‡,§,#] Shaul Aloni,[⊥] Virginia Altoe,[⊥] Nasim Alem,[†,‡,§] Cağlar Girit,[†,‡] Baisong Geng,[†,∥] Lorenzo Maserati,[†,¶] Michael Crommie,[†,‡,§] Feng Wang,[†,‡,§] and A. Zettl[†,‡,§,*]

[†]Department of Physics, University of California at Berkeley, Berkeley, California 94720, [‡]Materials Sciences Division, Lawrence Berkeley National Laboratory, Berkeley, California 94720, [§]Center of Integrated Nanomechanical Systems (COINS), Berkeley, California 94720, [⊥]The Molecular Foundry, Lawrence Berkeley National Laboratory, Berkeley, California 94720, [∥]School of Physical Science and Technology, Lanzhou University, Lanzhou 730000, China, and [¶]Politecnico di Milano, 20133 Milano, Italy. [#]These authors contributed equally to this work.

ABSTRACT We demonstrate a process for batch production of large-area (100−3000 μm^2) patterned free-standing graphene membranes on Cu scaffolds using chemical vapor deposition (CVD)-grown graphene. This technique avoids the use of silicon and transfers of graphene. As one application of this technique, we fabricate transmission electron microscopy (TEM) sample supports. TEM characterization of the graphene membranes reveals relatively clean, highly TEM-transparent, single-layer graphene regions (~50% by area) and, despite the polycrystalline nature of CVD graphene, membrane yields as high as 75−100%. This high yield verifies that the intrinsic strength and integrity of CVD-grown graphene films is sufficient for sub-100 μm width membrane applications. Elemental analysis (electron energy loss spectroscopy (EELS) and X-ray energy-dispersive spectroscopy (EDS)) of the graphene membranes reveals some nanoscaled contamination left over from the etching process, and we suggest several ways to reduce this contamination and improve the quality of the graphene for electronic device applications. This large-scale production of suspended graphene membranes facilitates access to the two-dimensional physics of graphene that are suppressed by substrate interactions and enables the widespread use of graphene-based sample supports for electron and optical microscopy.

KEYWORDS: suspended graphene membrane · atomically thin membrane · graphene TEM grids · TEM · CVD graphene · EELS · EDS

Many of the predicted properties arising from the two-dimensional nature of graphene[1−4] can be obscured or altered by perturbations caused by an interaction with an underlying substrate.[5] Therefore, interest and effort have heightened for the preparation of suspended graphene structures to ascertain graphene's fundamental properties[6−16] and explore nanomechanical[17,18] and electronic[9,13,19] applications not possible with substrate-bound graphene. However, current techniques used to produce suspended graphene membranes are underdeveloped and generally not scalable. These techniques rely on low-yield, serial processes typically involving the transfer of optically identified exfoliated graphene[1] or graphene grown on metal substrates[20,21] to a perforated substrate,[8] such as a commercial transmission electron microscopy (TEM) grid,[19,22] or to a substrate for additional microfabrication processing (*i.e.*, patterned metal deposition, etching, *etc.*) to produce a suspended membrane.[6,7] In any case, optical identification is a meticulous process, even for the trained eye, which together with the delicate nature of graphene transfer precludes the possibility of wafer-scale fabrication.

In this report, we present a scalable, economical, and parallel process for the fabrication of graphene membranes suspended over lithographically patterned Cu scaffolds without the use of silicon, commercial sample supports (*i.e.*, TEM grids), or any graphene transfer steps. Our process produces high-quality single-layer graphene membranes in high yield (>75%) with controllable diameters ranging from 20 to 60 μm, which are ideally suited for use as support structures to study other atomic and nanoscale materials,[23] systems,[24,25] and dynamics using electron[7,16,23] and optical[12] microscopy and spectroscopy. Furthermore, this work establishes the strength and stability of suspended CVD-grown graphene films in large-area membrane applications and permits further characterization of this important new material.

RESULTS AND DISCUSSION

Our suspended graphene membrane fabrication process (Scheme 1) begins with low-pressure chemical vapor deposition (CVD) of methane and hydrogen to grow graphene on 10 and 25 μm thick Cu foils as described by Li *et al.*[21] Since the CVD process coats both sides of the foil with graphene, we remove the graphene from one side of the Cu foil using an oxygen reactive ion etch and cover both sides of the foil with positive photoresist. A photomask with the desired dark-field pattern is placed

*Address correspondence to azettl@berkeley.edu.

Received for review March 6, 2010 and accepted June 29, 2010.

Published online July 6, 2010. 10.1021/nn100459u

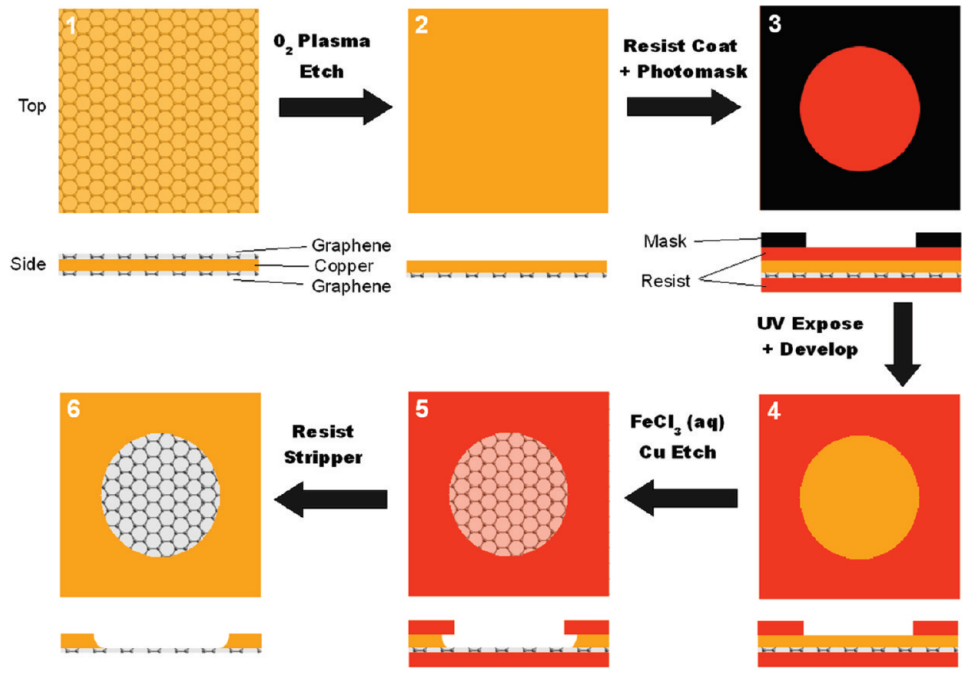

Scheme 1. Process flow diagram for transfer-free suspended graphene membrane fabrication on Cu. The top and bottom of each image corresponds to the plan view and side view of the substrate, respectively. (1) CVD synthesized graphene grown on Cu. (2) Graphene from one side of Cu is removed with an oxygen plasma etch, and (3) both sides of the substrate are coated in photoresist. Conventional photolithography is used to pattern the resist on the Cu side of the substrate to (4) expose the mask-defined regions of the Cu. (5) A ferric chloride solution etches the Cu down to the underlying graphene/resist. The remaining photoresist is stripped resulting in (6) a patterned, suspended graphene membrane.

over the resist/Cu side of the substrate, which is then given an appropriate UV exposure followed by immersion in wet developer. The resulting exposed patterned regions of the Cu surface are then etched by submersing the foil in an aqueous solution of $FeCl_3$, which is lightly agitated with a small stir rod. The etching process is complete when the etch reaches the graphene, approximately 7 min for 10 μm thick Cu foils and 20 min for 25 μm thick Cu foils. Longer etching times cause the hole diameters to further dilate, and local variations in foil thickness and solution agitation lead to some variation in hole diameters (see Figure 1b,c). Finally, the patterned foil is thoroughly rinsed in deionized water to remove traces of the etchant, immersed in hot acetone (60 °C) to strip photoresist, rinsed in isopropyl alcohol, and allowed to air-dry.

As a proof-of-concept, we fabricate conventional TEM sample supports (TEM "grids") consisting of a ~3.1 mm diameter Cu disk with suspended graphene spanning a centered 9 × 9 array of patterned circular holes (Figure 1b). After fabrication, the sample supports remain connected to the foil by two small tabs that can be cut to free the TEM grid. The area of the Cu foils used in this work was limited by the inner-tube radius of CVD quartz tubes to about 2 cm^2, which generated four loosely spaced TEM grids. The total substrate real estate of a TEM grid is about 0.1 cm^2, so using a tighter spacing than was used in this work could produce as many as 20 TEM grids per 2 cm^2 foil. With larger diameter tube furnaces or by inserting rolls of Cu sheets into a furnace, our process could be used with much larger area foils to produce thousands of graphene-based TEM sample supports on a single 100 cm^2 foil. This increase in yield is a several orders-of-magnitude improvement over conventional serial preparation of graphene TEM grids.

The quality and crystallinity of the graphene membranes is characterized using high-resolution TEM and electron beam diffraction. We find that approximately 50% of the graphene surface is covered with islands of amorphous material (see Supporting Information), which is similar to earlier reports on graphene TEM grid preparation.[23] Many membranes are fully intact or have tears that remove only 5−35% of membranes, as can be seen in Figure 1d, although tear-free membranes are more prevalent when their width is on the order of 15 μm or less. In Figure 1d, the graphene sheet is made visible at low magnification by small Cu particles left by an incomplete etch. Despite the contamination shown in Figure 1d, the sample is often highly clean on the nanoscopic scale, with atomically clean single-layer graphene regions on the order of 10^4 nm^2, as shown in Figure 1e. We note that these atomically clean regions are as large as or larger than have been previously reported,[6,7,19,22,23] and that the Cu particulate contamination can be further abated with a post-etch HCl bath. Electron diffraction analysis (Figure 1f) in such clean regions of the membranes indicates that it has the hexagonal crystal structure of graphene's honeycomb lattice, though additional rotated diffraction

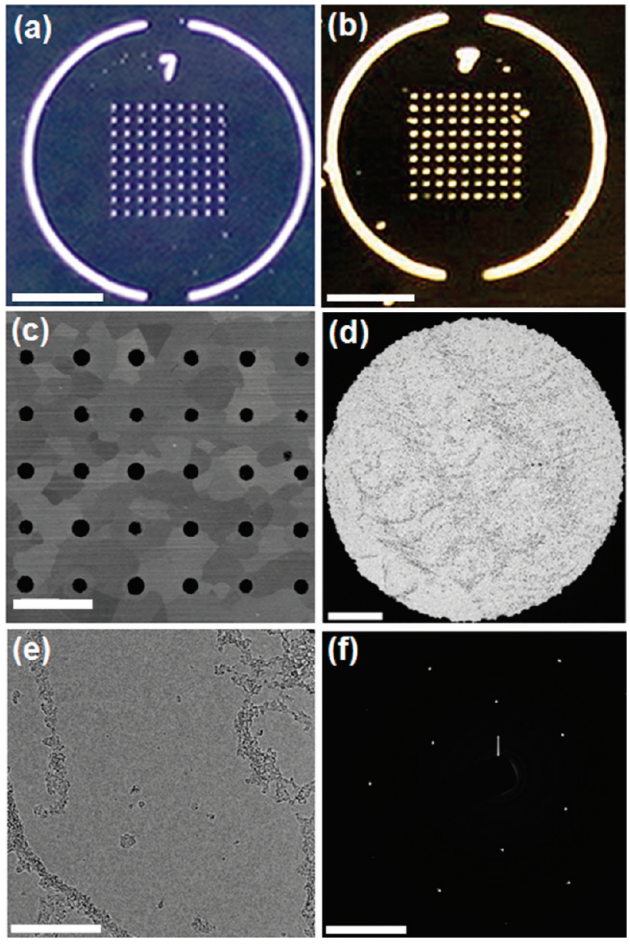

Figure 1. Lithographically defined graphene TEM sample supports. (a) One of the repeating elements of the photomask used to create an array of TEM grids (scale bar: 1 mm). (b) Back-side illuminated optical image of ~3.1 mm diameter TEM grid produced using the procedure outlined in Scheme 1 with the photomask from (a). The Cu tabs can be cut with a razor blade to remove the grid to be used in a conventional TEM sample stage. The patterned "7" indicates the graphene side of the grid (scale bar: 1 mm). (c) Scanning electron micrograph shows etched holes and Cu grains on 25 μm thick foils (scale bar: 200 μm). (d) TEM of a 55 μm diameter graphene membrane. Cu nanoparticles left from an incomplete etching process help visualize the graphene. A small tear in the lower left side of the membrane contrasts vacuum with clean regions of the membrane (scale bar: 10 μm). (e) Higher magnification TEM of a large clean region of a graphene membrane with sparse amorphous contamination (scale bar: 50 nm). (f) Selected area electron diffraction pattern of the membrane, confirming the known hexagonal crystal structure of graphene (scale bar: 5 nm^{-1}).

spots do appear in some regions, which suggest the presence of complex lattice orientations, most likely from multiple graphene grains or graphene multilayers intersecting the beam path. Furthermore, we observe a weak monotonic character of the diffraction peak intensities with tilt angle, which establishes the suspended regions as mostly single-layer graphene, in accord with Meyer *et al.*[6]

The transparency of clean single-layer graphene is evident from Figure 2a, which shows a membrane near a region of free space. The image's grayscale intensity distribution in regions of graphene (red dot/curve in Figure 2a,b) closely resembles regions of free space (blue dot/curve in Figure 2a,b). The shift from vacuum and broadness of the intensity distribution of the amorphous regions (gray dot/curve in Figure 2a,b) is similar to that of commercial amorphous carbon and Si_3N_4 thin-film sample supports and makes it difficult to image low-contrast entities such as biological molecules or low atomic number elements. Graphene's relatively narrow intensity bandwidth and well-defined crystallinity thus enable TEM and diffraction of low contrast objects.

The yield of intact graphene membranes depends strongly on the hole diameter. For 30−60 μm diameter holes (area ~ 1000−3000 μm^2), we were able to attain yields—that is, regions of intact suspended graphene—of 75% using 25 μm thick foil, while nearly all of the membranes on the 10 μm thick foils had failed. However, when hole diameters are reduced to about 20 μm (area ~300 μm^2), the 10 μm thick foil yield improves to ~60% and the 25 μm thick foil yield surpasses 90%. For hole diameters $\lesssim$15 μm, we observe that both 10 and 25 μm thick foils produce intact graphene membranes nearly 100% of the time. The yield's dependence on foil thickness may be related to the disparate Cu grain sizes seen in the 10 and 25 μm thick foils, a result of different foil manufacturing conditions. We found that the annealed (post-graphene growth) 10 and 25 μm thick Cu foils have grains on the order of 10 and 100−1000 μm^2, respectively, as can be seen from the SEM micrographs in Figure 1c for the 25 μm thick foil. Smaller Cu grains may lead to smaller graphene domains and/or a higher graphene "wrinkle" density, producing weaker graphene films which are more easily destroyed during wet processing. Previous work[6,7] on exfoliated single-crystal graphene generated membranes up to several tens of micrometers in width by using critical point drying techniques. We note here that suspended CVD-grown polycrystalline graphene survives rather harsh wet chemical etching and drying without the use of critical point techniques, confirming not only the robustness of single grains but also the interaction strength between adjacent grains.

Variations in hole diameter are mainly caused by the isotropic nature of the $FeCl_3$ etch, which under ideal conditions (precise timing, controlled etchant concentration and temperature, uniform fluid agitation, *etc.*) would lead to radial dilation equal to the Cu foil thickness—thus, suspended graphene regions with a diameter equal to the mask-defined diameter plus twice the Cu foil thickness. Non-uniform fluid agitation (especially near the resist etch mask) causes non-uniformities across the foil, with smaller features often being under-etched. Since we used large, uniformly etched features as a visual gauge to cease etching, we often observe unusually low dilation in the array of small suspended graphene regions. As shown in Figure 1c, we see dilation of approximately 21 ± 5 μm

compared to the 50 μm diameter dilation expected for 25 μm thick Cu foils, in addition to the 15 μm diameter holes defined by the photomask. Variations in the foil thickness, determined by atomic force microscopy (see Supporting Information), have a negligible contribution to the overall hole diameter variations. Also, scanning electron micrographs of hole undersides (see Supporting Information) show that the etched pits of the Cu are not smooth but contain grains as large as 3 μm in diameter; this roughness can also be seen in the edges of the membrane shown in Figure 1d. This roughness puts a lower bound on the size of suspended graphene regions that can be reproducibly fabricated with this technique. However, a slightly more complex microfabrication pathway would lead quite easily to more precisely defined suspended structures. For example, by the appropriate use of a thin-film material and its corresponding etchant (*e.g.*, silicon dioxide/HF), one could define a secondary support scaffold with features approaching the current limitations of photolithography or electron beam lithography.

The method described above is a general technique for the fabrication of suspended graphene membranes by directly etching the underlying copper support of CVD-grown graphene. For some applications, such as for TEM imaging, the membranes can be used directly, while for others, such as for sensing or electronic device applications,[26] it may be desirable to reduce certain kinds of surface contamination. Therefore, it is instructive to know what contaminants remain following the etch process. Figure 3a is a color-contrast TEM micrograph showing graphene (orange) with a typical amount of amorphous carbon contamination (yellow/light green) and evidence of a polycrystalline contaminant (blue/green). High-resolution TEM of this contamination is shown in Figure 3b and illustrates its crystallinity. We obtain an elemental fingerprint of the contamination through the use of electron energy loss spectroscopy (EELS) and X-ray energy-dispersive spectroscopy (EDS) in a TEM. Spectroscopic analysis was performed in regions with contamination similar to that shown in Figure 3a,b. EELS data (Figure 3c) reveal the presence of carbon, oxygen, and iron in our sample with an approximate atomic ratio (C/O/Fe) of 5:3:1. EDS data (Figure 3d) confirm the existence of carbon, oxygen, and iron but also detected small amounts of copper and chlorine. The atomic percentages determined through EDS are as follows: C (55%), O (32%), Fe (12%), Cl (1%), and Cu (<1%). The Cl, Cu, and some of the Fe are likely left over from the etching and may be in the form of $FeCl_3$, copper oxides, copper chlorides, or more complex compounds. However, the high concentration of Fe and O relative to Cl and the correlation of their locations suggest that some of the Fe from the etchant has formed an oxide and has produced the nanosized crystals on the graphene surface seen in Figure 3b. Rinsing the samples in a solution that can dissolve iron oxide (acetic acid, citric acid, *etc.*) may remove part of this contamination. To avoid the formation of iron oxides altogether, one could also employ alternative Cu etchants such as sodium persulfate, ammonium persulfate, or organic acids such as citric, glycolic, acetic, malic, and oxalic acids.[27]

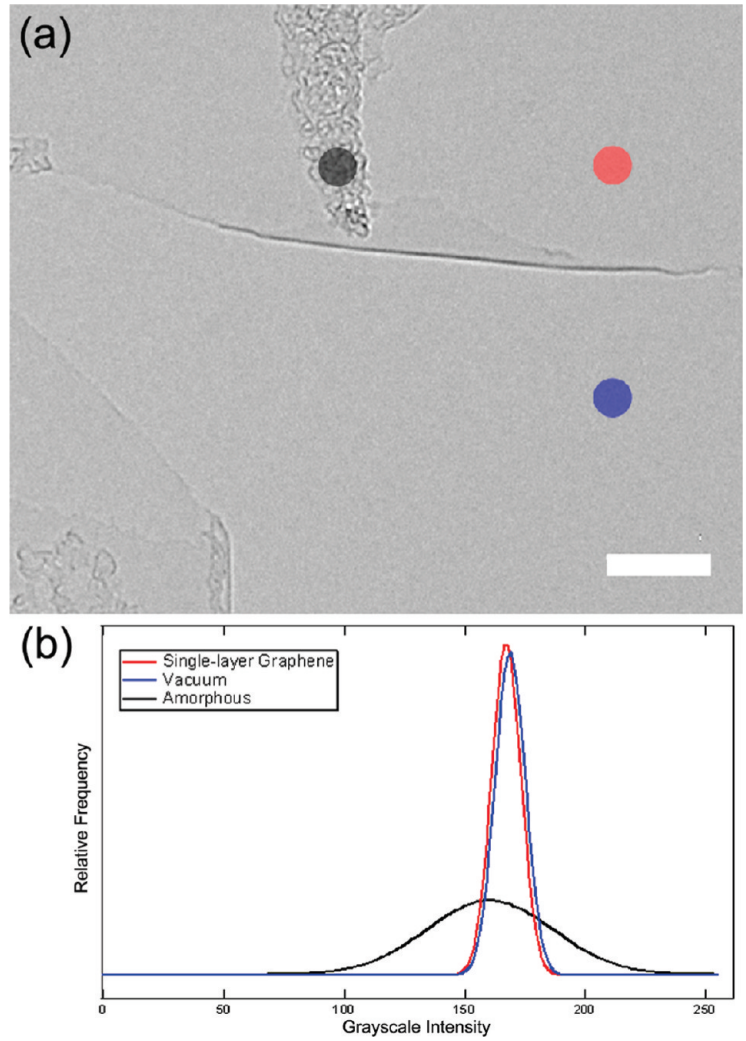

Figure 2. TEM transparency of graphene membranes. (a) Clean regions of single-layer graphene (red dot) near a tear in the membrane are compared to vacuum (blue dot) and amorphous debris (black dot) (scale bar: 10 nm). (b) Grayscale intensity distributions of single-layer graphene (red curve), vacuum (blue curve), and amorphous (black curve) regions. The graphene and vacuum have nearly indistinguishable contrast signatures, while the amorphous region's distribution is shifted and much broader. This contrast difference makes graphene far superior to amorphous carbon in resolving low-contrast entities.

In conclusion, we have demonstrated a process for the batch fabrication of Cu-supported, large-area graphene membranes, which shows that CVD-grown graphene has sufficient robustness to form suspended membranes comparable in size to the

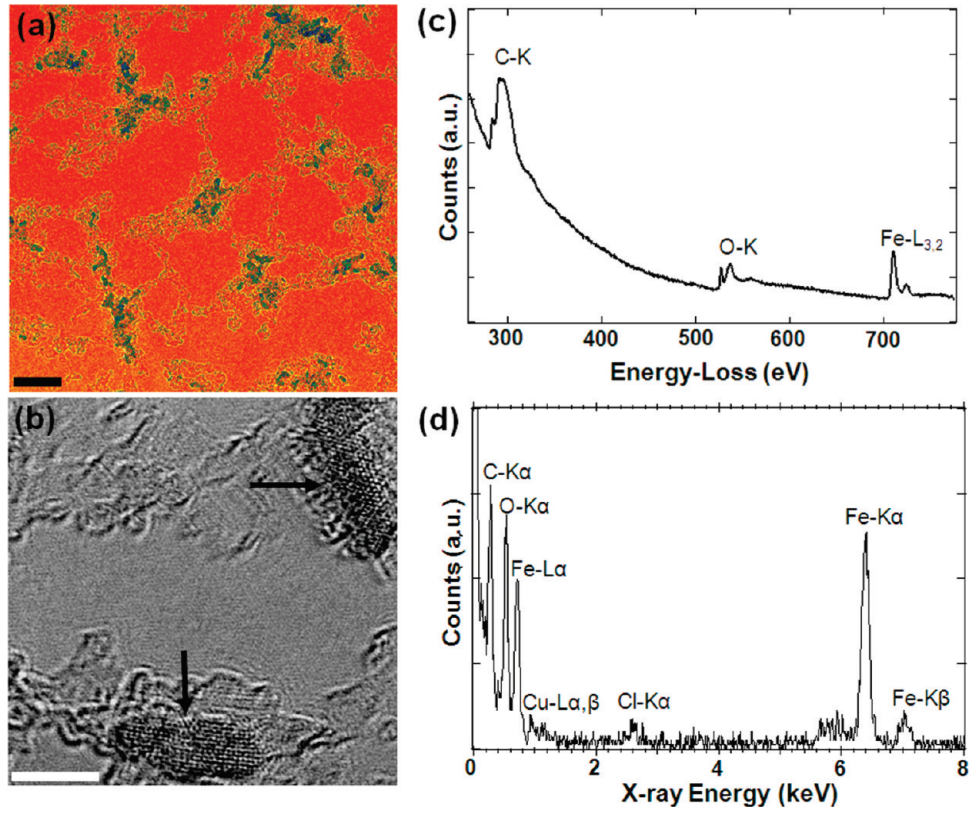

Figure 3. TEM and elemental microanalysis of iron-containing contamination on the surface of $FeCl_3$-etched CVD graphene. (a) Color-contrast TEM micrograph showing regions of pristine graphene (orange-yellow), amorphous carbon (yellow-light green), and iron-containing contaminant (dark green-blue) (scale bar: 20 nm). (b) High-resolution TEM of iron-containing contamination (scale bar: 5 nm). (c) Electron energy loss spectroscopy (EELS) data and (d) X-ray energy-dispersive spectroscopy (EDS) data obtained from sample regions containing contamination similar to that shown in (a) and (b). EELS data clearly show the presence of carbon, oxygen, and iron. X-ray spectroscopy data confirm the presence of carbon, oxygen, and iron but also show traces of copper and chloride.

largest produced using exfoliated, single-crystal graphene.[7] This process is a significant enabling step for further optical, mechanical, electronic, and thermal experimentation on graphene and can be made compatible with other graphene growth substrates such as Ni,[20,28] Pt,[29] and Ir.[30] Also, we used this process to produce graphene-based TEM sample supports in high yield that provide superior contrast enhancement over commercially available thin-film (a-C, Si_3N_4, *etc.*) supports, which opens up the possibility of wafer-scale production of graphene-based TEM grids. The well-defined crystal structure of these membranes facilitates their use as a metrological diffraction standard and, when used as a sample support, permits the straightforward removal of graphene's diffraction signal from electron beam or X-ray diffraction of other materials. Elemental analysis (EELS and EDS) of the membrane surface, which reveals that an iron oxide contaminant can be left over after the etching process, provides important insight for the use of CVD-grown graphene in applications such as sensing and electronics. Since sufficient inertial clamping is provided by the copper support, our method can be utilized to produce suspended graphene-based nanoelectromechanical systems which, due to graphene's extraordinary stiffness[7] and strength,[11] low mass, and large surface-to-volume ratio, could provide optically probed[17] ultrahigh resolution force, mass, and charge sensors.[7,31] With appropriate processing (potentially involving the transfer of the etched graphene/Cu foil to an insulating substrate) to decouple the graphene from the copper support and thus avoid shorting, one could use these suspended graphene films for electrical measurements and applications. In addition, these membranes show promise for separating or filtering between two different environments.

METHODS

Graphene Membrane Fabrication. Large-area polycrystalline graphene films are grown on Cu using low-pressure chemical vapor deposition described by Li *et al.*[21] Briefly, 10 or 25 μm thick Cu foils (99.8% Alfa Aesar, Ward Hill, MA) are loaded into a CVD furnace and evacuated to a base pressure of ~50 mTorr under a steady 2 sccm flow of H_2 gas. The furnace is ramped up to 1000 °C over 30 min, and then CH_4 gas is introduced at 35 sccm for 30

min during which graphene growth occurs. The furnace is then allowed to cool, and the graphene is removed. A reactive ion etcher (Plasma Etch, Inc., USA) is used with 50 sccm of O_2 at 50 W for 20 s to remove the top-side graphene. About 1 μm of resist (Rohm & Haas Megaposit SPR 955-CM-0.9, MicroChem Corp., Newton, MA) is spun onto substrates at ~2000 rpm and baked at 110 °C for 90 s, then masked and exposed with a ~175 mJ/cm^2 i-Line dose. The substrates are post-baked at 110 °C for 90 s and then developed in 1−3.5% TMAH (OPD 4262, Arch Chemicals, USA) for 60 s followed by Cu etching in a 0.1 g/mL aqueous solution of iron(III) chloride hexahydrate (ACS reagent grade 97%, Sigma-Aldrich, USA), which is lightly agitated using a stir bar at 200 rpm. The sample is then rinsed in deionized water to remove traces of the etchant, immersed in hot acetone (60 °C) to strip photoresist, rinsed in isopropyl alcohol, and allowed to air-dry.

Electron Microscopy. High-resolution transmission electron microscopy (HRTEM) and selected-area electron diffraction were performed with a JEOL 2010 microscope operated at 100 keV and a JEOL 2100-F operated at 120 keV. A single-tilt stage at room temperature and a liquid nitrogen anti-contamination device were used in both microscopes. X-ray spectrometry (INCAEnergyTEM 250, Oxford) and electron energy loss spectroscopy (Tridiem, Gatan) were performed at 120 keV in a JEOL 2100-F. Scanning electron microscopy (SEM) was performed in an FEI Sirion (FEI Company, USA) operated at 5 keV.

Acknowledgment. We thank B. Kessler for technical assistance, and G. Dour and J. Weldon for discussion. This work was supported in part by the Office of Naval Research MURI program under Grant N00014-09-1-1066, which provided for the development of the fabrication method. Growth facilities and high-resolution analytical TEM were provided by the Director, Office of Energy Research, Lawrence Berkeley National Lab Materials Sciences and Engineering Division, of the U.S. Department of Energy under Contract No. DE-AC02-05CH11231 through the sp^2-bonded Materials Program and the Molecular Foundry's user program. Microscopy and diffraction characterization were also provided by the National Science Foundation through the Center of Integrated Nanomechanical Systems under Grant No. EEC-0832819 and through Grant No. DMR 0906539. B.A. acknowledges support from the UC Berkeley A.J. Macchi Fellowship Fund in the Physical Sciences. W.R. acknowledges support through a National Science Foundation Graduate Research Fellowship, and B.G. acknowledges support from the China Scholarship Council.

Supporting Information Available: Additional TEM of graphene membranes, atomic force microscopy of Cu surfaces, and SEM of back-side of etched features. This material is available free of charge *via* the Internet at http://pubs.acs.org.

REFERENCES AND NOTES

1. Novoselov, K. S.; Geim, A. K.; Morozov, S. V.; Jiang, D.; Zhang, Y.; Dubonos, S. V.; Grigorieva, I. V.; Firsov, A. A. Electric Field Effect in Atomically Thin Carbon Films. *Science* **2004**, *306*, 666–669.
2. Novoselov, K. S.; Jiang, D.; Schedin, F.; Booth, T. J.; Khotkevich, V. V.; Morozov, S. V.; Geim, A. K. Two-Dimensional Atomic Crystals. *Proc. Natl. Acad. Sci. U.S.A.* **2005**, *102*, 10451–10453.
3. Geim, A. K.; Novoselov, K. S. The Rise of Graphene. *Nat. Mater.* **2007**, *6*, 183–191.
4. Neto, A. H. C.; Guinea, F.; Peres, N. M. R.; Novoselov, K. S.; Geim, A. K. The Electronic Properties of Graphene. *Rev. Mod. Phys.* **2009**, 109–162.
5. Zhang, Y. B.; Brar, V. W.; Girit, C.; Zettl, A.; Crommie, M. F. Origin of Spatial Charge Inhomogeneity in Graphene. *Nat. Phys.* **2010**, *6*, 74.
6. Meyer, J. C.; Geim, A. K.; Katsnelson, M. I.; Novoselov, K. S.; Booth, T. J.; Roth, S. The Structure of Suspended Graphene Sheets. *Nature* **2007**, *446*, 60–63.
7. Booth, T. J.; Blake, P.; Nair, R. R.; Jiang, D.; Hill, E. W.; Bangert, U.; Bleloch, A.; Gass, M.; Novoselov, K. S.; Katsnelson, M. I.; Geim, A. K. Macroscopic Graphene Membranes and Their Extraordinary Stiffness. *Nano Lett.* **2008**, *8*, 2442–2446.
8. Bunch, J. S.; Verbridge, S. S.; Alden, J. S.; van der Zande, A. M.; Parpia, J. M.; Craighead, H. G.; McEuen, P. L. Impermeable Atomic Membranes From Graphene Sheets. *Nano Lett.* **2008**, *8*, 2458–2462.
9. Du, X.; Skachko, I.; Barker, A.; Andrei, E. Y. Approaching Ballistic Transport in Suspended Graphene. *Nat. Nanotechnol.* **2008**, *3*, 491–495.
10. Frank, I. W.; Tanenbaum, D. M.; van der Zande, A. M.; McEuen, P. L. Mechanical Properties of Suspended Graphene Sheets. *J. Vac. Sci. Technol., B* **2007**, *25*, 2558–2561.
11. Lee, C.; Wei, X. D.; Kysar, J. W.; Hone, J. Measurement of the Elastic Properties and Intrinsic Strength of Monolayer Graphene. *Science* **2008**, *321*, 385–388.
12. Nair, R. R.; Blake, P.; Grigorenko, A. N.; Novoselov, K. S.; Booth, T. J.; Stauber, T.; Peres, N. M. R.; Geim, A. K. Fine Structure Constant Defines Visual Transparency of Graphene. *Science* **2008**, *320*, 1308.
13. Bolotin, K. I.; Sikes, K. J.; Jiang, Z.; Klima, M.; Fudenberg, G.; Hone, J.; Kim, P.; Stormer, H. L. Ultrahigh Electron Mobility in Suspended Graphene. *Solid State Commun.* **2008**, *146*, 351–355.
14. Bolotin, K. I.; Ghahari, F.; Shulman, M. D.; Stormer, H. L.; Kim, P. Observation of the Fractional Quantum Hall Effect in Graphene. *Nature* **2009**, *462*, 196–199.
15. Du, X.; Skachko, I.; Duerr, F.; Luican, A.; Andrei, E. Y. Fractional Quantum Hall Effect and Insulating Phase of Dirac Electrons in Graphene. *Nature* **2009**, *462*, 192–195.
16. Girit, C. O.; Meyer, J. C.; Erni, R.; Rossell, M. D.; Kisielowski, C.; Yang, L.; Park, C. H.; Crommie, M. F.; Cohen, M. L.; Louie, S. G.; Zettl, A. Graphene at the Edge: Stability and Dynamics. *Science* **2009**, *323*, 1705–1708.
17. Bunch, J. S.; van der Zande, A. M.; Verbridge, S. S.; Frank, I. W.; Tanenbaum, D. M.; Parpia, J. M.; Craighead, H. G.; McEuen, P. L. Electromechanical Resonators from Graphene Sheets. *Science* **2007**, *315*, 490–493.
18. Garcia-Sanchez, D.; van der Zande, A. M.; Paulo, A. S.; Lassagne, B.; McEuen, P. L.; Bachtold, A. Imaging Mechanical Vibrations in Suspended Graphene Sheets. *Nano Lett.* **2008**, *8*, 1399–1403.
19. Meyer, J. C.; Girit, C. O.; Crommie, M. F.; Zettl, A. Hydrocarbon Lithography on Graphene Membranes. *Appl. Phys. Lett.* **2008**, *92*, 3.
20. Kim, K. S.; Zhao, Y.; Jang, H.; Lee, S. Y.; Kim, J. M.; Ahn, J. H.; Kim, P.; Choi, J. Y.; Hong, B. H. Large-Scale Pattern Growth of Graphene Films for Stretchable Transparent Electrodes. *Nature* **2009**, *457*, 706–710.
21. Li, X. S.; Cai, W. W.; An, J. H.; Kim, S.; Nah, J.; Yang, D. X.; Piner, R.; Velamakanni, A.; Jung, I.; Tutuc, E.; Banerjee, S. K.; Colombo, L.; Ruoff, R. S. Large-Area Synthesis of High-Quality and Uniform Graphene Films on Copper Foils. *Science* **2009**, *324*, 1312–1314.
22. Park, H. J.; Meyer, J.; Roth, S.; Skakalova, V. Growth and Properties of Few-Layer Graphene Prepared by Chemical Vapor Deposition. *Carbon* **2010**, *48*, 1088–1094.
23. Meyer, J. C.; Girit, C. O.; Crommie, M. F.; Zettl, A. Imaging and Dynamics of Light Atoms and Molecules on Graphene. *Nature* **2008**, *454*, 319–322.
24. Meyer, J. C.; Kisielowski, C.; Erni, R.; Rossell, M. D.; Crommie, M. F.; Zettl, A. Direct Imaging of Lattice Atoms and Topological Defects in Graphene Membranes. *Nano Lett.* **2008**, *8*, 3582–3586.
25. Gass, M. H.; Bangert, U.; Bleloch, A. L.; Wang, P.; Nair, R. R.; Geim, A. K. Free-Standing Graphene at Atomic Resolution. *Nat. Nanotechnol.* **2008**, *3*, 676–681.
26. Levendorf, M. P.; Ruiz-Vargas, C. S.; Garg, S.; Park, J. Transfer-Free Batch Fabrication of Single Layer Graphene Transistors. *Nano Lett.* **2009**, *9*, 4479–4483.
27. Pernel, C.; Farkas, J.; Louis, D. Copper in Organic Acid Based Cleaning Solutions. *J. Vac. Sci. Technol., B* **2006**, *24*, 2467–2471.

28. Reina, A.; Jia, X. T.; Ho, J.; Nezich, D.; Son, H. B.; Bulovic, V.; Dresselhaus, M. S.; Kong, J. Large Area, Few-Layer Graphene Films on Arbitrary Substrates by Chemical Vapor Deposition. *Nano Lett.* **2009**, *9*, 30–35.
29. Land, T. A.; Michely, T.; Behm, R. J.; Hemminger, J. C.; Comsa, G. STM Investigation of Single Layer Graphite Structures Produced on Pt(111) by Hydrocarbon Decomposition. *Surf. Sci.* **1992**, *264*, 261–270.
30. Coraux, J.; N'Diaye, A. T.; Busse, C.; Michely, T. Structural Coherency of Graphene on Ir(111). *Nano Lett.* **2008**, *8*, 565–570.
31. Craighead, H. G. Nanoelectromechanical Systems. *Science* **2000**, *290*, 1532–1535.